



Targeting Cyclin B1 with Antisense Oligonucleotides- Coated Superparamagnetic Iron Oxide Nanoparticles

Hosam Zaghloul^{1*}, Doaa A. Shahin¹, Ibrahim El-Dosoky³, Mahmoud E. El-awady⁴, Fardous F. El-Senduny⁵,
Nashwa K. Abousamra¹, Farid A. Badria²

¹ Clinical Pathology Department, Faculty of Medicine, Mansoura University, Egypt

² Pharmacognosy Department, Faculty of Pharmacy, Mansoura University, Egypt

³ Pathology Department, Faculty of Medicine, Mansoura University, Egypt

⁴ Zoology Department, Faculty of Science, Mansoura University, Egypt

⁵ Chemistry Department, Faculty of Science, Mansoura University, Egypt

Article Info: Received 24 September 2018; Accepted 22 October. 2018

Cite this article as: Zaghloul, H., Shahin, D. A., Dosoky, I. E., El-awady, M. E., El-Senduny, F. F., Abousamra, N. K., & Badria, F. A. (2018). TARGETING CYCLIN B1 WITH ANTISENSE OLIGONUCLETOTIDES- COATED SUPERPARAMAGNETIC IRON OXIDE NANOPARTICLES. *Journal of Drug Discovery And Therapeutics*, 6(10).

DOI: <https://doi.org/10.32553/jddt.v6i10.444>

Address for Correspondence: Prof. Dr. Farid A. Badria, *Pharmacognosy Department, Faculty of Pharmacy, Mansoura University, Egypt*

Disclosure statement: *The authors have no conflicts of interest.*

ABSTRACT

Antisense oligonucleotides (ASO) represent an attractive trend as specific targeting molecules but sustain poor cellular uptake meanwhile superparamagnetic iron oxide nanoparticles (SPIONs) offer stability of ASO and improved cellular uptake. In the present work we aimed to functionalize SPIONs with ASO targeting the mRNA of Cyclin B1 which represents a potential cancer target and to explore its anticancer activity. For that purpose, four different SPIONs-ASO conjugates, S-M (1–4), were designated depending on the sequence of ASO and constructed by crosslinking carboxylated SPIONs to amino labeled ASO. The impact of S-M (1–4) on the level of Cyclin B1, cell cycle, ROS and viability of the cells were assessed by flowcytometry. The results showed that S-M3 and S-M4 reduced the level of Cyclin B1 by 35 and 36%, respectively. As a consequence to downregulation of Cyclin B1, MCF7 cells were shown to be arrested at G2/M phase (60.7%). S-M (1–4) led to the induction of ROS formation in comparison to the untreated control cells. Furthermore, S-M (1–4) resulted in an increase in dead cells compared to the untreated cells and SPIONs-treated cells. In conclusion, targeting Cyclin B1 with ASO-coated SPIONs may represent a specific biocompatible anticancer strategy.

INTRODUCTION

Breast cancer is the most common malignancy among women and in Egypt is considered as the most prevalent cancer and constitutes 32% according to national cancer institute cases ¹. Ionizing radiation, exogenous hormones and alcohol beverages are considered the main reasons for breast cancer development ². Despite advances in the field of cancer therapy, surgery remains the

most effective treatment where the main bulk of tumor is removed ³. On the other hand, targeted therapies, like Imatinib, led to a significant shift in the treatment of cancer because it overcomes limitations of conventional chemotherapy like high toxicity and drug resistance. However, there is still a need to discover new safe and effective therapy against breast cancer.

Antisense oligonucleotides (ASO) represent an attractive trend in the development of targeted cancer therapies where more than 90 ASO-based drugs targeting cancer are in different phases of clinical trials⁴. Unlike conventional chemotherapeutics, ASO interact with its target in a high specific manner⁵ and block the translation of a targeted mRNA, for oncogenes or their regulatory pathways, into its corresponding protein; either through steric hindrance or through degradation⁶. Since all cancer cells are characterized by high level of Cyclin B1 expression to proceed through mitosis (G2/M transition), it may be a potential target for ASO based therapeutics. However, delivery of ASO remains unresolved issue, because it sustain poor cellular uptake.

Super paramagnetic iron oxide nanoparticles (SPIONs) have been employed in various cancer-related applications including; delivery of chemo- and bio-therapeutics, magnetic hyperthermia, controlled drug release and magnetic resonance imaging (MRI)^{7, 8}. In addition, SPIONs combine the functionality of therapy and diagnosis (Theranostics or Theragnosis) which is considered as a milestone in the development of personalized cancer therapy where the tumor can be imaged, treated and monitored for the treatment efficacy⁹. Despite being negatively charged, coupling of ASO to SPIONs overcome many challenges related to ASO delivery including; stabilization in physiological environments, protection from nuclease degradation, enhanced cellular uptake without using auxiliary reagents and prolonged intracellular half-life^{10, 11}. The aim of this work is to evaluate the anticancer activity of SPIONs coated with Cyclin B1-specific antisense oligonucleotids against breast cancer.

MATERIALS AND METHODS

Antisense Oligonucleotides (ASO):

Antisense DNA sequences specific for Cyclin B1 mRNA were designed using the *Sfold* web server (<http://sfold.wadsworth.org/cgi-bin/soligo.pl>) which provides computational tools for designing RNA-targeting nucleic acids, including antisense oligonucleotides (ASO)¹². Accession number of

human Cyclin B1 used for *Sfold* analysis was (NM_031966). Selection criteria were as follows; $40\% \leq GC\% \leq 60\%$, no GGGG in the target sequence, average unpaired probability for target site nucleotides ≥ 0.5 , Antisense oligo binding energy ≤ -8 kcal/mol. Selected ASO were modified with an amino group at 5' end (for crosslinking with SPIONs) and designated as shown in **Table (1)**.

Super Paramagnetic Iron Oxide Nanoparticles (SPIONs):

SPIONs were purchased from Ocean NanoTech, LLC (USA) in the form of Maghemite (Fe_2O_3), 10 nm diameter, suspended in water, autoclaved and functionalized by a surface carboxylic group. The concentration of iron (mg/ml) was determined by the following equation; Iron Concentration = $(OD_{500\text{ nm}} - OD_{800\text{ nm}}) \times \text{dilution factor} \times \text{Extinction coefficients}$; Where extinction coefficient was 4.3 for iron oxide nanoparticles of 10 nm size.

Conjugation of SPIONs with ASO:

Coupling of ASO to SPIONs was performed using the EDC/NHS chemistry as previously described¹³. Briefly, 200 μL of SPIONs (5 mg/ml) were re-suspended in a tube containing 100 μL dH_2O and the carboxylic groups were activated by 100 μL of EDC/NHS Mixture (EDC=2 mg/ml; NHS= 1 mg/ml) for 15 min. at RT with continuous mixing. Then, 400 μL dH_2O and 150 μL of ASO (100 μM) were added to the activated SPIONs and the reaction was incubated for 2 hrs at RT with continuous mixing. The resulting SPIONs-ASO conjugates (designated S-M1) were exposed to a magnetic field overnight and washed with 300 μL dH_2O and finally re-suspended in 300 μL dH_2O and stored at 4°C for future use. The same procedures were applied for M2 and M3 giving rise to S-M2 and S-M3 conjugates. In addition, the same protocol was applied to coat SPIONs with a mixture of the three ASO (M1, M2 and M3) at (50 μL of each) and the resulting conjugates were designated S-M4 (**Fig. 1**).

Characterization of SPIONs-ASO conjugates

FT-IR (Nicolet iS10 FT-IR Spectrometer, Thermo Scientific) was used to detect the formation of amide bond between carboxylated SPIONs and the amino-labeled ASO. In addition, Z-potential and the

hydrodynamic diameter of SPIONs (S), activated SPIONs (A.S) and SPIONs-ASO (S-M1-4) conjugates were measured by Malvern Zetasizer Nano-zs90 (Malvern instruments Ltd., UK).

Cell Culture

Human Breast cancer cell line (MCF-7) was purchased from American Type Culture Collection (ATCC). The cells were cultivated at 37°C and 5% CO₂ in DMEM (Dulbecco's modified eagle medium) (Lonza, 12-604F) medium supplemented with 10% fetal bovine serum (FBS, Lonza, 14-801E) and 100 IU/ml penicillin and 100 µg/ml streptomycin (Lonza, 17-602E).

Viability/ Cytotoxicity of SPIONs-ASO

LIVE/DEAD assay (Molecular Probes, L3224) was used to evaluate the cytotoxicity of SPIONs-ASO conjugates according to the manufacturer instructions. Briefly, 5*10⁶ cells/ml were collected by trypsinization and suspended in 1 ml PBS (pH=7.4). After that, collected cells were stained with 2 µl (50 µM) calcein AM and 4 µl (2 mM) ethidium homodimer-1 for 15 min in dark at room temperature. Stained cells were counted by flow cytometry at excitation/emission 488/530 nm for calcein and 488/610 for ethidium homodimer-1.

Cellular uptake of SPIONs-ASO conjugates

Iron content of treated MCF7 cells was visualized by using the Prussian blue stain (Sigma Aldrich™, Cat. No HT20). Briefly, cells were seeded on coverslip in 24-well plate and incubated overnight at 37°C and 5% CO₂ before replacing the medium with new medium containing SPIONs-ASO at a concentration of 2 mg/ml of iron. After 48 hours of incubation, the cells were washed two times with 1x PBS to remove excess SPIONs and fixed with working iron staining solution for 10 minutes then washed by dH₂O and counterstained in working pararosaniline solution followed by washing with dH₂O and air dried.

Effect of SPIONs-ASO conjugates on Cyclin B1 level

The ability of SPIONs-ASO conjugates to interfere with Cyclin B1 mRNA was evaluated by treatment of MCF7 cell line with concentration of S-M1-4 corresponding to 2 mg Fe/ml for 48 hours. Then the level of Cyclin B1 as a protein product was measured

by flow cytometry. Briefly, cells were washed with 1x PBS and collected after trypsinization. After 2x washing with 1x PBS, the cells were fixed and permeabilized by 500 µl/of Cytofix/Cytoperm solution (BD Bioscience™, Cat. No. 554714) for 20 min at 4°C. Then, cells were stained by the FITC Cyclin B1 Antibody (BD Pharmingen™, Cat. No. 554108) for 1 hours then washed two times with 1x PBS to remove the excess stain. The level of cyclin B1 was detected by analyzing the samples within one hour by using BD FACSCanto II (BD Bioscience™) Unstained cells and cells stained with FITC Mouse IgG₁, κ Isotype were used as controls.

Cell cycle analysis:

The ability of SPIONs-ASO conjugates to induce growth arrest was evaluated by determination of DNA content in each phase by using propidium iodide. The cells were treated as mentioned above and collected after trypsinization followed by washing with 1x PBS and fixed for 2 hours at -20°C with Ice-cold absolute ethanol. Then fixed cells were washed with 1x PBS and re-suspended in 200 µl of propidium iodide (50 µg/ml, 556463) and incubated for 15 min at RT followed by analysis by using BD FACSCanto II (BD Bioscience™).

Determination of the level of Reactive Oxygen Species (ROS)

Cellular ROS level was monitored using the DCFDA Cellular ROS Detection Assay (Abcam®, ab113851) according to the manufacturer instructions. Briefly, MCF-7 cells were seeded in a 24-well plate (5x10⁴ cells/well) and allowed to attach for 16 hrs. Then, cells were stained with 20 µM DCFDA and incubated for 30 minutes at 37°C. Then cells were treated with 2 mg/ml of iron content of SPIONs-ASO for 6 hrs. Cells were analyzed by flowcytometry (BD FACSCanto II, BD Bioscience™) at excitation/emission 488/535 nm, respectively.

RESULTS

Characterization of the SPIONs-ASO conjugate

The commercial SPIONs in the present study were coated with oleic acid to produce particles bearing ~ 100 carboxylic acid groups for each particle. FT-IR (KBr) showed peaks characteristic for carboxylic acid

group (3449 Cm^{-1} , 1645 Cm^{-1}) (**Fig. 2A**). Upon conjugation of the carboxylated SPIONs and the amino labeled ASO, the amide was formed. This was confirmed using FT-IR (KBr) which showed stretching peaks at 1638 Cm^{-1} and 1650 Cm^{-1} (**Fig. 2B**).

On the other hand the average hydrodynamic diameter as determined by dynamic light scattering (DLS) revealed an increased size after crosslinking the ASO to the SPIONs as shown in **Table 2**.

Detection of SPIONs

The cellular uptake of SPIONs-ASO conjugates was assessed histologically by using Prussian blue assay which depends on the interaction of acidified ferrocyanide with any Fe^{3+} ions in the cells to give the bright blue stain called Prussian blue. After 48 hours of treatment of the cells with either SPIONs alone or SPIONs-ASO, the Prussian blue pigment was high in the cells treated with SPIONs-ASO (63% stained cells) in comparison to SPIONs-treated cells (26% stained cells) (**Fig. 3**). This assay confirmed the internalization of SPIONs-ASO to the breast cancer cells.

Cytotoxicity of SPIONs-ASO

In order to determine the cytotoxic activity of SPIONs-conjugated to cyclin B1 mRNA antisense oligonucleotides (S-M1-4) against breast cancer cells, the cells were either treated with SPIONs alone or SPIONs-ASO for 48 hours then the percent of viable and dead cells was determined by staining the cells with Ethidium homodimer-1 and Calcein AM. Ethidium homodimer-1 indicates the dead cells with damaged plasma membrane and binds to the DNA while Calcein AM is used as an indicator for the viability of the cells through indirect detection of esterase enzyme activity. (**Fig. 4**) showed the increase in the dead cells after treating the cells with SPIONs-ASO, S-M (1-4), in comparison to the untreated cells and SPIONs-treated cells. This shows the anticancer activity of SPIONs-ASO conjugates to breast cancer cells. This led to further analysis for the level of cyclin B1 in treated cells.

SPIONs-ASO downregulate translation of Cyclin B1

After treating breast cancer cells with SPIONs-ASO conjugates for 48 hours, the cells were collected, fixed and permeabilized to determine the level of intracellular cyclin B1 protein. It was found that, S-M3 and S-M4 were able to inhibit cyclin B1 mRNA translation and led to 35 and 36% reduction, respectively, in the level of cyclin B1 in the treated breast cancer cells (**Fig. 5**).

SPIONs-ASO induce cell cycle arrest

Cyclin B1 in conjugation with cyclin-dependent kinases regulate the transition of the cells from G2 to M phase via promotion of chromosome condensation, retraction of the nuclear envelope, assembly of the mitotic spindle apparatus, and alignment of condensed chromosomes at the metaphase plate. So the decrease in cyclin B1 level in the cells will lead to cell cycle arrest at G2/M phase.

In order to investigate and confirm this hypothesis, the DNA content in each cycle of SPIONs-ASO conjugates-treated breast cancer cells was measured by staining the cells with propidium iodide. As shown in **Fig. 6**, the cells treated with SPIONs-ASO conjugates were arrested at G2/M phase.

SPIONs-ASO induce ROS formation

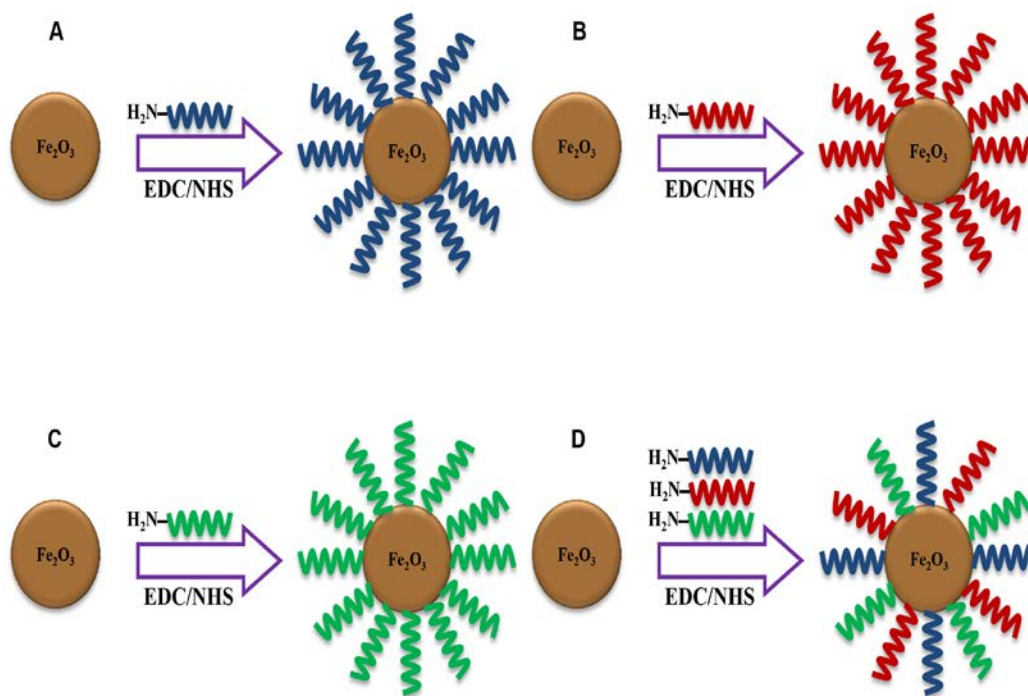
It is well known that the iron oxide nanoparticles induce the formation of reactive oxygen species (ROS) such as hydroxyl radicals (OH^{\cdot}) via Fenton reaction. ROS attacks lipids and form malondialdehyde which is considered as mutagenic due to the formation of adducts with deoxyguanosine, deoxyadenosine or deoxycytidine bases. Based on these facts, the level of ROS in the treated breast cancer cells was measured by using 2',7'-dichlorofluorescein diacetate (DCFDA). This fluorogenic dye diffuses through the cell membrane and deacytalyated by esterases to non-fluorescent dye which is oxidized by cellular ROS to give the fluorogenic product 2', 7'-dichlorofluorescein (DCF). As it is in **Fig. 7**, SPIONs-ASO conjugates led to the induction of ROS production in the cells that were treated with S-M (1-4) in comparison to the untreated control cells.

Table 1: Selected sequences targeting Cyclin B1 mRNA.

| ASO name | Sequence |
|----------|--|
| M1 | 5`-H ₂ N-C6-GTGCTTTGTAAGTCCTTGAT-3` |
| M2 | 5`-H ₂ N-C6-GAATTCAGCTGTGGTAGAGT-3` |
| M3 | 5`-H ₂ N-C6-GCAGAATTCAGCTGTGGTAG-3` |

Table 2: Hydrodynamic diameter and Z-potential measurements.

| | Size (nm) | Z-potential (mV) |
|-------------|--------------|------------------|
| S | 42.12 ± 1.85 | -63.4 ± 0.89 |
| A.S | 41.18 ± 0.51 | -57.2 ± 1.63 |
| S-M1 | 58.75 ± 3.20 | -32.12 ± 1.95 |
| S-M2 | 55.33 ± 1.90 | -33.20 ± 2.26 |
| S-M3 | 56.54 ± 2.17 | -31.90 ± 2.38 |
| S-M4 | 59.00 ± 2.36 | -31.08 ± 2.04 |

**Fig. 1:** Schematic representation for SPIONs-ASO conjugates. A, S-M1; B, S-M2; C, S-M3; S-M4

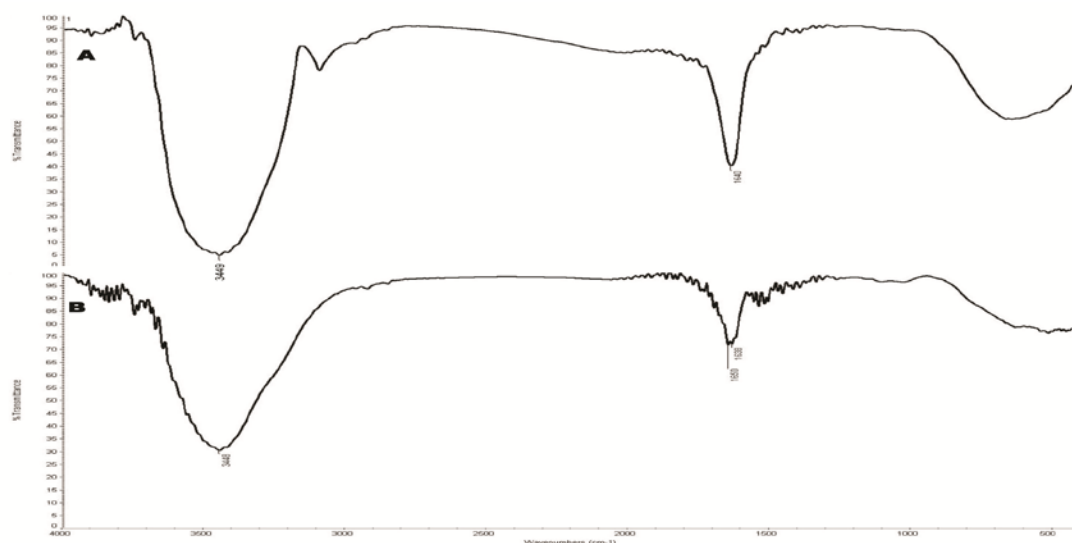


Fig. 2: FT-IR confirmed the coupling between carboxylated SPIONs and amino group in ASO. (A) SPIONs (B) ASPIONs-ASO

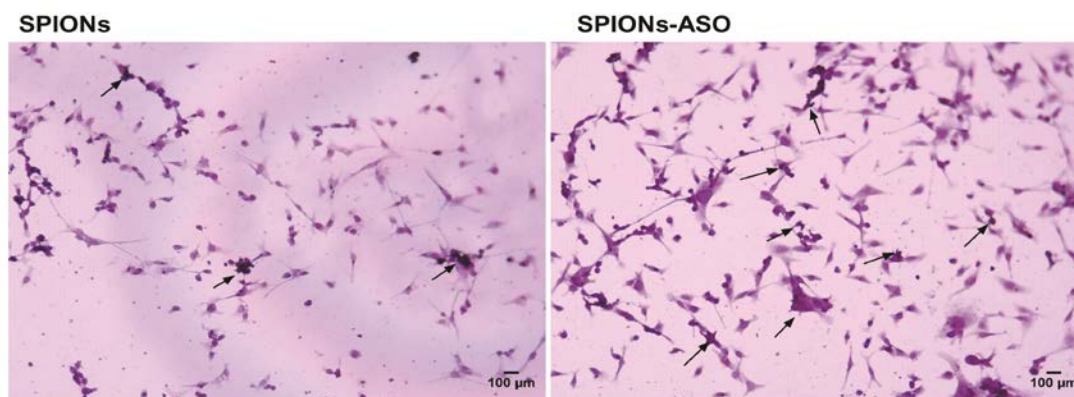


Fig. 3: Cellular uptake of SPIONs-ASO conjugates for targeting cyclin B1 mRNA. The fixed cells were stained with Prussian blue working solution. Iron-containing cells showed blue stain (Black arrow).

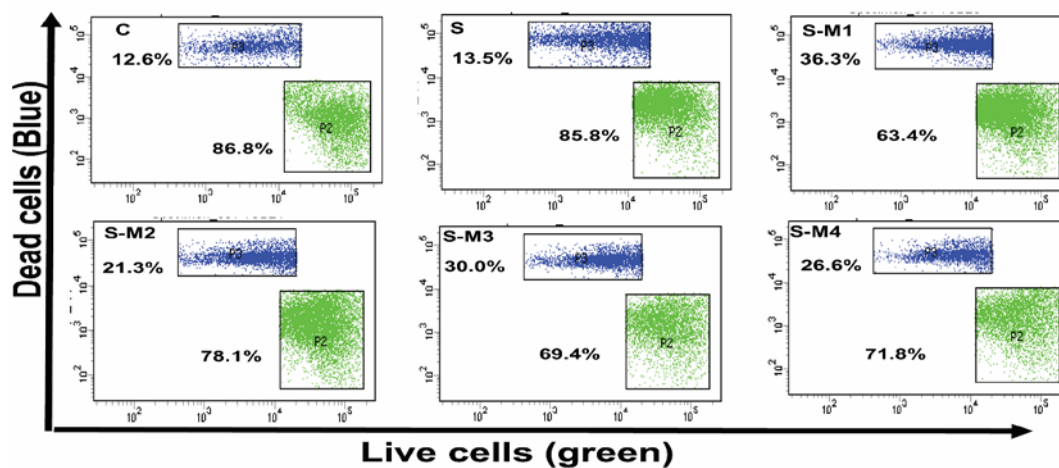


Fig. 4: SPIONs-ASO conjugates increased the dead breast cancer cells. C, control; S, SPIONs; S-M (1–4), SPIONs-ASO conjugates 1–4.

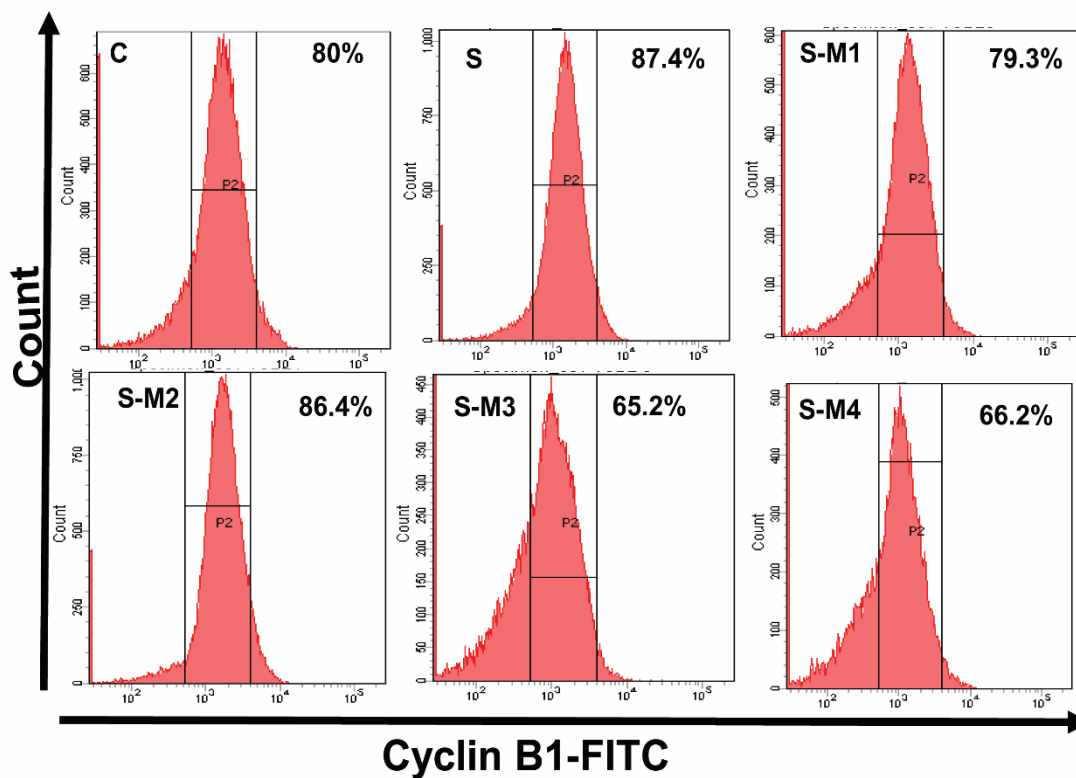


Fig. 5: SPIONs-ASO conjugates targeted cyclin B1 mRNA and decreased the level of cyclin B1 protein. C, control; S, SPIONs; S-M (1–4), SPIONs-ASO conjugates 1–4.

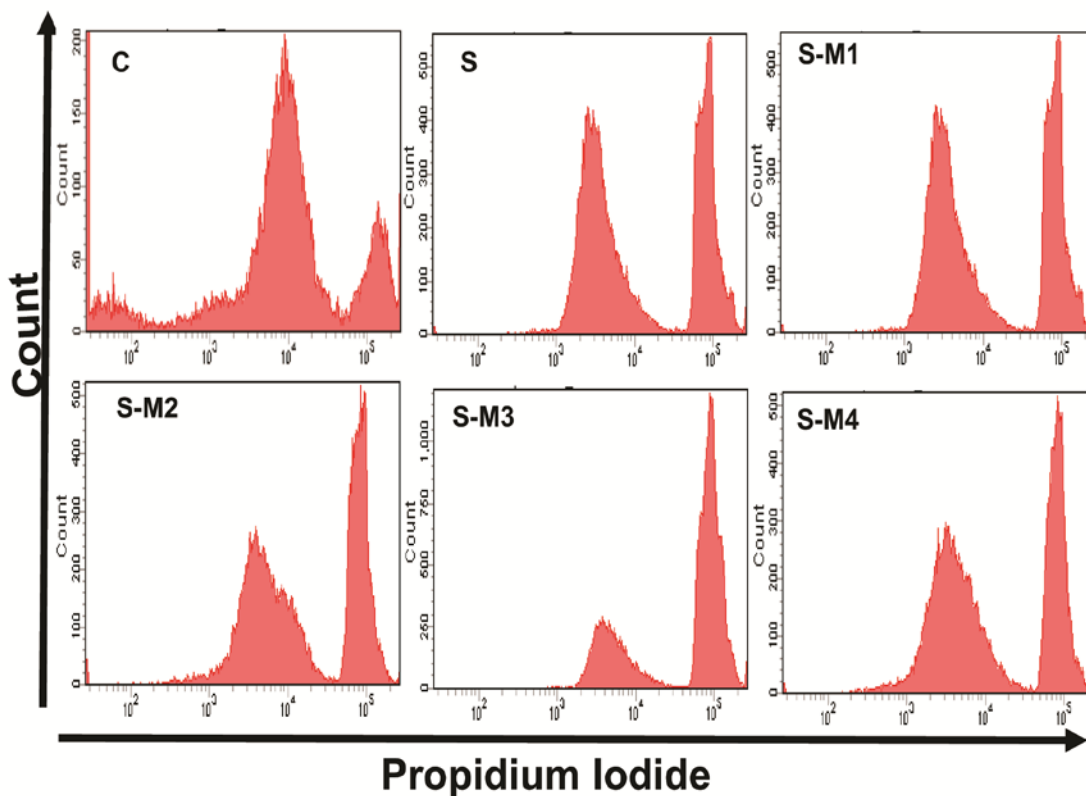


Fig. 6: Cell cycle arrest at G2/M phase after targeting Cyclin B1 by SPIONs-ASO.

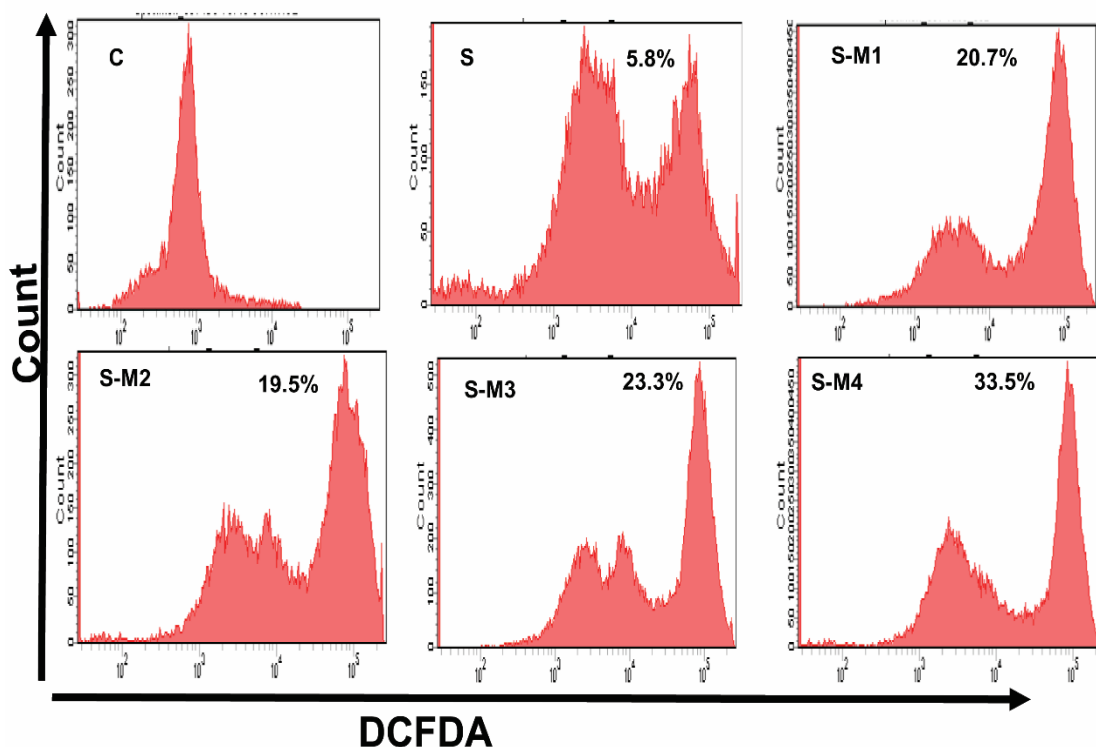


Fig. 7: A significant increase in the production of ROS in response to SPIONs-ASO conjugates treatment. C, control; S, SPIONs; S-M (1–4), SPIONs-ASO conjugates 1–4.

DISCUSSION

SPIONs-based delivery of nucleic acids became a well document approach where it have been employed for the delivery of antisense oligonucleotides (ASO)^{14, 15}, small interfering RNA (siRNA) and plasmid DNA (pDNA)¹⁶. In addition, SPIONs were found to be efficient for the delivery of ASO into difficult-to-transfect cells like the human umbilical vein endothelial cells (HUVEC) under external magnetic field giving rise to a transfection method termed magnetofection¹⁷. Another way for the delivery, is coupling of negatively charged SPIONs with positively labelled antisense oligonucleotides. It is reported that each bead can be loaded with 70 oligos¹⁸.

In the present work, coupling of SPIONs to ASO was found to improve cellular uptake of SPIONs (63%) as compared to uncoated SPIONs (26%) (**Fig. 3**). The cellular uptake of ASO-modified particles increase by increasing the density of ASO where serum proteins¹⁰ play role in the adsorption process followed by the recognition by scavenger receptors, class of pattern recognition receptors (PRRs)¹⁹. Calero *et al* 2015

showed that the internalization mechanism depends on the size of the aggregates where the smaller one will be internalized via clathrin-dependent pathway while the bigger one will be through micropinocytosis²⁰.

There is discrepancies in the reported cytotoxicity of SPIONs and this may be explained by the differences in the cell line and the experimental conditions^{21, 22}. For instance, Calero *et al* reported that, all cellular parameters including cell morphology, focal adhesion, cytoskeletal components, cell cycle, cell viability and ROS formation was not affected in SPIONs-treated MCF-7 cells²⁰, in agreement with our results. On the other hand, Alarifi *et al* 2014, showed that SPIONs induced morphological changes, ROS production, mitochondrial damage, breakage in DNA strands leading to apoptosis in MCF-7²³. Moreover, even commercially available SPIONs that share the same chemical characteristics as size and coating²², showed differences in the cytotoxic effect against different cell lines where in our study, SPIONs were not cytotoxic to MCF-7 (**Fig. 4**) but toxic to HeLa cells in another study¹³.

Cyclin B1 is considered as a potential target in cancer therapy for many reasons. Firstly, it is a key regulator in mitosis²⁹. Secondly, it has been documented to be overexpressed in many types of tumors and its overexpression is correlated with tumor progression and poor prognosis³⁰. Thirdly, targeting it was found to induce growth arrest and apoptosis *in vitro* and *in vivo*^{31, 32}. In the present work, S-M3 and S-M4 reduced the level of Cyclin B1 by 35 and 36%, respectively (**Fig. 5**) accompanied with cell cycle arrest (**Fig. 6**). To our knowledge, it is the first time to use SPIONs-ASO for targeting Cyclin B1. To enhance targeting efficiency, ASO can be designed containing multiple binding sites for the targeted mRNA (i.e have the ability to bind to different regions in the targeted mRNA)³³. However, in the present work S-M4 which has multitargeting sequences did not show improved results over S-M3 that has unitargeting sequence. Also, variation in the activity of S-M (1–4) can be explained by difference in the secondary structure of targeted region which is known to influence the efficacy of interfering-based approaches³⁴.

All SPIONs-ASO in the present work, S-M (1–4), led to the induction of ROS in comparison to the untreated control cells (**Fig. 7**). It is well documented that, ROS interacts with macromolecules leading to lipid peroxidation, protein denaturation and DNA double strand breaks, damage different cellular components (cytoskeleton, mitochondria and chromosomes) and alter cell functions (signaling, gene expression and cell cycle) leading to ultimate cell death^{22, 24-27}. In general, cytotoxicity of SPIONs is hypothesized to arise at higher concentrations (higher than 100 $\mu\text{g Fe /ml}$)²⁷. However, at low concentrations, increased ROS formation and DNA damage may be observed even in the absence of cytotoxicity²⁸.

The present SPIONs-ASO (S-M3) may be also used as an adjuvant therapy where SPIONs were shown to boost the action of β -lapachone, a hydrogen peroxide releasing substance, with 10-fold ROS generation and significant cell death over those of β -lapachone only³⁵. In another study, SPIONs were shown to sensitize MCF-7 cells to doxorubicin when a static magnetic field was applied³⁶. Furthermore,

treatment of MCF-7 cells with Taxol after knockdown of Cyclin B1 by siRNA showed a significant reduction in cell number and induced growth arrest at G2/M in addition to a robust apoptotic response³⁷. The combination of CyclinB1 siRNA with Daunorubicin led to an increased apoptotic response in HepG2 cells, compared to cells treated with Daunorubicin alone, in a dose dependent manner. In addition, the combination showed a selective anticancer activity over the HL-7702 normal human liver cell lines³⁸. Since overexpression of Cyclin B1 was found to correlate with resistance to radiotherapy³⁹, downregulation of Cyclin B1 was found to enhance irradiation efficacy leading to growth arrest at G2/M and induced apoptosis³⁷.

In conclusion, SPIONs-ASO conjugates, S-M (1–4), targeting mRNA of Cyclin B1 were constructed and shown to have two synergetic actions; ASO downregulate the translation of Cyclin B1 mRNA into its corresponding protein, whereas SPIONs induce ROS formation. In turn, SPIONs-ASO conjugates may be a good candidate in the development of specific anticancer therapeutics with minimal toxicity.

Acknowledgment

This work was supported by Science and Technology Development Fund (STDF), Egypt, under Grant ID 4773.

REFERENCES

1. Ibrahim, A.S., et al., *Cancer incidence in Egypt: results of the national population-based cancer registry program*. Journal of cancer epidemiology, 2014. **2014**.
2. MacMahon, B., *Epidemiology and the causes of breast cancer*. Int J Cancer, 2006. **118**(10): p. 2373-8.
3. Urruticochea, A., et al., *Recent advances in cancer therapy: an overview*. Current pharmaceutical design, 2010. **16**(1): p. 3-10.
4. Castanotto, D. and C.A. Stein, *Antisense oligonucleotides in cancer*. Current opinion in oncology, 2014. **26**(6): p. 584-589.
5. Moreno, P.M. and A.P. Pêgo, *Therapeutic antisense oligonucleotides against cancer:*

- hurdling to the clinic*. *Frontiers in chemistry*, 2014. **2**.
6. Bennett, C.F. and E.E. Swayze, *RNA targeting therapeutics: molecular mechanisms of antisense oligonucleotides as a therapeutic platform*. *Annual review of pharmacology and toxicology*, 2010. **50**: p. 259-293.
 7. Revia, R.A. and M. Zhang, *Magnetite nanoparticles for cancer diagnosis, treatment, and treatment monitoring: recent advances*. *Materials Today*, 2016. **19**(3): p. 157-168.
 8. Majidi, S., et al., *Magnetic nanoparticles: Applications in gene delivery and gene therapy*. *Artificial cells, nanomedicine, and biotechnology*, 2016. **44**(4): p. 1186-1193.
 9. Shahbazi, R., B. Ozpolat, and K. Ulubayram, *Oligonucleotide-based theranostic nanoparticles in cancer therapy*. *Nanomedicine*, 2016. **11**(10): p. 1287-1308.
 10. Giljohann, D.A., et al., *Oligonucleotide loading determines cellular uptake of DNA-modified gold nanoparticles*. *Nano letters*, 2007. **7**(12): p. 3818-3821.
 11. Brigger, I., C. Dubernet, and P. Couvreur, *Nanoparticles in cancer therapy and diagnosis*. *Advanced drug delivery reviews*, 2002. **54**(5): p. 631-651.
 12. Ding, Y., C.Y. Chan, and C.E. Lawrence, *S fold web server for statistical folding and rational design of nucleic acids*. *Nucleic acids research*, 2004. **32**(suppl_2): p. W135-W141.
 13. Eustaquio, T. and J.F. Leary, *Nanobarcoded superparamagnetic iron oxide nanoparticles for nanomedicine: Quantitative studies of cell-nanoparticle interactions by scanning image cytometry*. *Cytometry Part A*, 2016. **89**(2): p. 207-216.
 14. Li, Y., et al., *Co-delivery of microRNA-21 antisense oligonucleotides and Gemcitabine using nanomedicine for pancreatic cancer therapy*. *Cancer Science*, 2017.
 15. Shen, H.-b., et al., *Magnetic force microscopy analysis of apoptosis of HL-60 cells induced by complex of antisense oligonucleotides and magnetic nanoparticles*. *Biophysical chemistry*, 2006. **122**(1): p. 1-4.
 16. Li, D., et al., *Theranostic nanoparticles based on bio-reducible polyethylenimine-coated iron oxide for reduction-responsive gene delivery and magnetic resonance imaging*. *International journal of nanomedicine*, 2014. **9**: p. 3347.
 17. Krötz, F., et al., *Magnetofection—a highly efficient tool for antisense oligonucleotide delivery in vitro and in vivo*. *Molecular Therapy*, 2003. **7**(5): p. 700-710.
 18. Geinguenaud, F.d.r., et al., *Easily controlled grafting of oligonucleotides on γ Fe₂O₃ nanoparticles: Physicochemical characterization of DNA organization and biological activity studies*. *The Journal of Physical Chemistry B*, 2014. **118**(6): p. 1535-1544.
 19. Patel, P.C., et al., *Scavenger receptors mediate cellular uptake of polyvalent oligonucleotide-functionalized gold nanoparticles*. *Bioconjugate chemistry*, 2010. **21**(12): p. 2250-2256.
 20. Calero, M., et al., *Characterization of interaction of magnetic nanoparticles with breast cancer cells*. *Journal of nanobiotechnology*, 2015. **13**(1): p. 16.
 21. Khan, M.I., et al., *Induction of ROS, mitochondrial damage and autophagy in lung epithelial cancer cells by iron oxide nanoparticles*. *Biomaterials*, 2012. **33**(5): p. 1477-1488.
 22. Lei, L., et al., *Toxicity of superparamagnetic iron oxide nanoparticles: research strategies and implications for nanomedicine*. *Chinese Physics B*, 2013. **22**(12): p. 127503.
 23. Alarifi, S., et al., *Iron oxide nanoparticles induce oxidative stress, DNA damage, and caspase activation in the human breast cancer cell line*. *Biological trace element research*, 2014. **159**(1-3): p. 416-424.
 24. Abdal Dayem, A., et al., *The role of reactive oxygen species (ROS) in the biological activities of metallic nanoparticles*. *International journal of molecular sciences*, 2017. **18**(1): p. 120.
 25. Dissanayake, N.M., K.M. Current, and S.O. Obare, *Mutagenic effects of iron oxide nanoparticles on biological cells*. *International journal of molecular sciences*, 2015. **16**(10): p. 23482-23516.

26. Mahmoudi, M., et al., *Assessing the in vitro and in vivo toxicity of superparamagnetic iron oxide nanoparticles*. Chemical reviews, 2011. **112**(4): p. 2323-2338.
27. Singh, N., et al., *Potential toxicity of superparamagnetic iron oxide nanoparticles (SPION)*. Nano reviews, 2010. **1**(1): p. 5358.
28. Jin, M., J.-C. Ryu, and Y.-J. Kim, *Investigation of the genetic toxicity by dextran-coated superparamagnetic iron oxide nanoparticles (SPION) in HepG2 cells using the comet assay and cytokinesis-block micronucleus assay*. Toxicology and Environmental Health Sciences, 2017. **9**(1): p. 23-29.
29. Gavet, O. and J. Pines, *Progressive activation of CyclinB1-Cdk1 coordinates entry to mitosis*. Developmental cell, 2010. **18**(4): p. 533-543.
30. Ye, C., et al., *Prognostic role of cyclin B1 in solid tumors: a meta-analysis*. Oncotarget, 2017. **8**(2): p. 2224.
31. Yuan, J., et al., *Cyclin B1 depletion inhibits proliferation and induces apoptosis in human tumor cells*. Oncogene, 2004. **23**(34): p. 5843-5852.
32. Yuan, J., et al., *Stable gene silencing of cyclin B1 in tumor cells increases susceptibility to taxol and leads to growth arrest in vivo*. Oncogene, 2006. **25**(12): p. 1753-1762.
33. Rubenstein, M., P. Tsui, and P. Guinan, *Antisense Oligonucleotides as Specific Chemotherapeutic Delivery Agents: A New Type of Bifunctional Antisense*.
34. Luo, K.Q. and D.C. Chang, *The gene-silencing efficiency of siRNA is strongly dependent on the local structure of mRNA at the targeted region*. Biochemical and biophysical research communications, 2004. **318**(1): p. 303-310.
35. Huang, G., et al., *Superparamagnetic iron oxide nanoparticles: amplifying ROS stress to improve anticancer drug efficacy*. Theranostics, 2013. **3**(2): p. 116.
36. Aljarrah, K., et al., *Magnetic nanoparticles sensitize MCF-7 breast cancer cells to doxorubicin-induced apoptosis*. World journal of surgical oncology, 2012. **10**(1): p. 62.
37. Androic, I., et al., *Targeting cyclin B1 inhibits proliferation and sensitizes breast cancer cells to taxol*. BMC cancer, 2008. **8**(1): p. 391.
38. ZHANG, Y., et al., *siRNA induced cyclinB1 knockdown sensitizes HepG2 cells to daunorubicin*. Progress in Biochemistry and Biophysics, 2011. **38**(6): p. 551-557.
39. Hassan, K.A., et al., *Cyclin B1 overexpression and resistance to radiotherapy in head and neck squamous cell carcinoma*. Cancer research, 2002. **62**(22): p. 6414-6417.